Modulated and intergrowth structures in minerals and electron microscope methods for their study

PETER R. BUSECK

Departments of Geology and Chemistry
Arizona State University
Tempe, Arizona 85287

AND JOHN M. COWLEY

Department of Physics
Arizona State University
Tempe, Arizona 85287

Abstract

Many minerals contain structural modulations that arise from cation site ordering, from slight positional displacements, or from a combination of both. Such fluctuations can be produced during crystal growth, cooling, spinodal decomposition, chemical reaction, or from other sorts of transformations. The effects are subtle and are commonly difficult to observe with many of the traditional mineralogical tools; this is especially true if some structural disorder also occurs. Related effects occur in minerals that contain intergrowths of different structure types on a unit cell scale.

Transmission electron microscopy, because of its high spatial resolution and its ability to image non-periodic features, is well adapted for the study of modulated crystals and intergrowth structures. High-resolution imaging permits direct observation of structural fluctuations, whereas electron diffraction provides a highly sensitive probe of larger regions as well as distinguishing between modulations resulting from displacive *vs.* substitutional effects. Microanalysis using the electron beam as a primary excitation source holds potential for detecting and measuring compositional differences across small regions, in some cases having dimensions comparable to modulation wavelengths. Electron beam instruments clearly are a powerful way for investigating the long-period structural complexities that occur in many minerals.

Introduction

Most mineral and many synthetic crystalline materials have traditionally been described by idealized crystal structures that are perfectly periodic and that can be adequately summarized by a regularly repeating unit cell. However, in many cases it is not possible to specify a unit cell that contains all of the essential features of the crystal. Examples include modulated structures, which are characterized by structural or chemical variations that repeat more or less regularly at spacings that are relatively large. These structures may be strictly or only statistically periodic, and the repeat distances are commonly greater than several tens of angstrom units in length. The number and variety of known structural modulations is large (*e.g.*, Cowley *et al.*, 1979). Many minerals exhibit such modulations; examples that we mention in this paper include silicates such as feldspar, pyroxene, and serpentine; sulfides such as pyrrhotite, digenite, and bornite; oxides such as hollandite and romanechite; as well as a selection of synthetic compounds that display a variety of modulations.

Modulated structures are important because they commonly are intermediate stages that form during the process of transformation from one structure to another or during the unmixing of one phase into several phases. Morimoto (1978) discusses several such examples. The modulations may represent either structural distortions or compositional changes or, in many cases, both. They thus are a means by which crystals can assume compositions or structures that are transitional between two or more different end members. Spinodal decomposition in pyroxenes, amphiboles, and feldspars pro-

vides examples. For those cases where they represent metastable intermediate steps, modulated structures can provide significant insight into the mechanisms of transformation. Modulated structures are also of interest since they provide a structural means for accommodating the small chemical changes required to produce non-stoichiometric phases.

Some of the unusual features of modulated structures can be explained as the result of statistical distributions of domains separated by out-of-phase boundaries. There are other long-period structures that involve two or more types of substructures that are recognizably different from each other. These can alternate in one or more dimensions with either a well defined regularity or one that is regular only in a statistical sense, i.e., when averaged over many units of substructure. We refer to these composites as "intergrowth structures," a term that is reasonably well established in the literature.[1] Both modulated and intergrowth structures have features such as superperiodicities in common, and the methods used to study them are similar. Therefore both are considered in this paper.

Although structural modulations and intergrowths can be considered theoretically, separate from diffraction data, a primary experimental source of information derives from diffraction measurements. For modulated structures the diffraction spots from the single substructure are usually strong, widely spaced, and sharply defined. The long-period modulations introduce satellite spots that are typically much weaker and more closely spaced. Disordered intergrowth structures can produce similar effects. In many cases, where the long-period structure is imperfectly ordered, the satellite spots may be less sharp or streaked in particular directions. In some cases, the spacings of these spots are non-integral submultiples of the substructure spacings, i.e., the substructure spots are not at rational multiples of the spot spacings resulting from the modulations or intergrowths. These structures are called incommensurate. Regularly spaced groups of such non-integral satellite spots, centered on different strong substructure spots, commonly overlap in an apparently uncorrelated manner. Small changes in composition or the conditions of crystallization may cause displacements of the satellite spots in a continuous fashion.

[1] An equivalent term that has found relatively wide usage in the mineralogical literature is "intercalation structure" or, for clays, "interstratification structure."

Much of the primary work on modulated and intergrowth mineral structures was done using single crystal X-ray measurements. However, one reason that these types of structure are not more familiar to noncrystallographers within the mineralogical community is that some of the standard methods used for the examination of minerals do not readily reveal the presence or suggest the nature of the modulations and intergrowths. Electron beam methods are much more effective in these respects. The presence and distributions of the satellite spots commonly are clearly seen in electron diffraction patterns and, in addition, high-resolution transmission electron microscopy can commonly provide an immediate picture of the nature of the modulations and intergrowths. Electron microscopy is often the only source of information on the nature of the faults locally perturbing the periodicity and on the interactions of these faults with other crystal defects.

A major goal of this paper is to demonstrate how electron-beam methods, especially high-resolution techniques, can be used to explore modulated and intergrowth structures, with selected examples from recent studies. We also suggest developments that may occur in the next few years and examine the sort of insights that these techniques will provide. Although we include a number of mineralogical examples, the emphasis is more on electron-beam techniques than on providing a thorough review of such structures in minerals. The latter can be found in Cowley et al. (1979) and the references therein.

Observational data are available from high-resolution images, electron diffraction patterns, and from microanalysis. These methods are discussed in sequence; clearly, microanalysis is useful only where compositional fluctuations occur. The other methods apply for any type of modulation. Where appropriate, imaging is useful for verification of the other, less direct methods. Whenever possible, all approaches are used.

Terminology and classification

The term "modulated structure" has been used with a wide variety of meanings; we use it to indicate that a basic periodic structure, called the substructure, is modified by a long-range modulation that has a periodicity that is greater than that of the substructure. The modulation may be (1) in the positions of the atoms, relative to the sublattice

(hollandite), or (2) in the occupancy of the various atomic sites (bornite–digenite), or both (intermediate plagioclase). In some cases, more than one modulation exists, but with different periodicities in different directions (pyrrhotite). The modulation may be a smoothly varying, almost sinusoidal displacement of atoms (antigorite—in the regions between the boundaries where the structure reverses sense). However, where a variation of site occupancy is involved, this cannot occur smoothly and continuously except on a statistical basis. In such instances the average occupancy of various sites in the sublattice may be smoothly modulated. Alternatively, the modulation may be produced by a statistical distribution of sharp discontinuities in the sublattice, such as out-of-phase domain boundaries; the average separation of the boundaries then defines the modulation periodicity (pyrrhotite).

The modulation may be commensurate or incommensurate. If it is commensurate, the modulation periodicity is an integral multiple of a sublattice periodicity. If, then, each atom displacement and the occupancy of each atomic site is defined within the unit cell of this long-range periodic structure, the modulation structure is indistinguishable from a superstructure, defined by a superlattice. In many cases, a structure that is commensurate at one temperature and pressure will become incommensurate at other conditions. In such cases, the modulation periodicity may vary continuously with the composition, the temperature, or some other parameter (e.g., tridymite; Dollase, 1967; Nukui, Yamamoto, and Nakazawa, 1979). Such modulations appear to be responses to an energy term operating independently of the factors determining the normal substructure (Cowley, 1979). For incommensurate structures, the long-range periodicity impressed on the substructure has no apparent special relationship to the substructure periodicity, i.e., the modulation is incommensurate with the sublattice.

In intergrowth structures the different substructures may intergrow in layers, chains, or other units and the different components may or may not fit together with a common periodicity. Where there is a misfit, the interface will show a periodically varying relationship of the substructures that may be commensurate (in so-called "vernier" structures) or incommensurate. In the following sections of this article we provide examples that illustrate the various types of both modulated and intergrowth structures. Table 1 summarizes some of the features characteristic of different types of modulat-

ed and intergrowth structures, their lattices, and selected diffraction characteristics.

There are some grey areas where the precise classification of a structure is not readily assigned. One such example is a commensurate structure with a periodicity several times greater than its constituent substructures, but where there is no evidence that the periodicity changes significantly with changes in temperature or pressure or limited atomic substitution. We shall consider these cases as ordered superstructures or, if they contain minor randomly distributed faults or intergrowths of a different structure, partially ordered superstructures rather than modulated structures.

For the intergrowth type of structures, we are particularly concerned with cases where a long-range periodicity is evident in the alternation of the components. There are examples, such as certain of the chain silicates of Veblen and Buseck (1979a) or the intergrowth tungsten bronzes of Sharma and Kihlborg (1981), for which regular intergrowths can occur; however, there are abundant cases in such materials where the regularity is not well defined and where the sequences may even appear to be entirely random. The reasons why the long-range periodicity should occur in some cases but not in others are far from clear. The evidence for the long-range periodicity is provided by either (1) a reasonable number of repetitions (at least 3, preferably more) of a sequence of units visible in high-resolution electron micrographs, or (2) well defined satellite spots representing the longer spacings in diffraction patterns. In the latter case, if there is a statistical distribution of the intergrowth substructures, the diffraction pattern may contain satellite spots at non-integral spacings, indicative of an incommensurate intergrowth structure.

Direct imaging of modulated structures

The use of high-resolution transmission electron microscopy for direct viewing with near-atomic resolution of crystal structures is well established and is particularly effective for studying the form of crystal defects. Provided that the crystal is sufficiently thin (less than 100Å for 100 keV electrons) and correctly oriented, the details of the perturbations of the structure can be seen, especially when the atom displacements involved are relatively large or when atoms of distinctly different atomic number are interchanged. In out-of-phase domain structures, for example, the discontinuity at each planar boundary is clearly seen, and the way in which the

Table 1. Correlations among structure types, existence of lattice, and selected diffraction features

Structure Type	Presence of:		Diffraction characteristics:	
	Single sublattice	Super-lattice	Non-integral spacings	High probability of diffuse spots or streaking
Fully-ordered substructure	✓[*]	X[*]	X	X
Fully-ordered superstructure	✓[**]	✓[**]	X	X
Partially-ordered superstructure	✓	✓	X	✓
Intergrowth structure				
Commensurate	X[+]	✓	X	(✓)
Incommensurate	X[+]	X	✓	✓
Modulated (non-intergrowth) structure				
Commensurate				
Statistical site occupation	X	✓	X	(✓)
Exact site occupation[++]	✓	✓	X	X
Incommensurate (modulation in site occupations or atom positions)	✓	X	✓	✓

[*] ✓ = yes; X = no; (✓) = generally yes.

[**]Although there is a theoretical problem with the existence of a sublattice once a superlattice is defined, we retain the terminology here to show the relationships among the several structure types.

[+]Multiple sublattices could be defined to correspond to each of the substructures, but they would lack the essential characteristic of "infinite" periodicity.

[++]Equivalent to the superstructures listed above unless it is one member of a series of mostly incommensurate structures.

separations of the boundaries vary around the average commensurate or incommensurate periodicity is evident.

In structures where the modulation takes the form of a periodicity of small atom displacements or small changes in atom scattering power, high-resolution images of thin crystals do not usually show sufficient contrast to make the modulation apparent, but considerable information can still be obtained at medium resolution (>10Å), especially for crystals that are too thick to be studied at highest resolutions. In such cases, it is common that the modulation becomes visible in thicker regions of the crystal (more than 100 to 200Å thick). This happens because strong dynamical scattering tends to enhance the effects of the small structural and chemical variations on the scattering amplitudes. Such images are difficult to interpret in terms of atom positions, but a great deal may be inferred about the modulations.

Out-of-phase domains and structural distortions

Many crystals contain several cations that have slightly different radii, but that occupy equivalent structural sites at high temperatures. Such disordered arrays can become increasingly unstable as the temperature decreases, and then the atoms commonly order in any of a variety of ways that relieve structural strain and that can result in modulations. Out-of-phase boundaries typically form during ordering, and they generally have relatively large displacement vectors (>1Å). (Anti-phase boundaries are a special case, where the displacement vector has exactly half the dimension of the unit cell in the direction of the displacement.) The distances between adjacent out-of-phase boundaries can vary, giving an average periodicity that may be commensurate or incommensurate.

The CuAu II alloy provides a simple example of an incommensurate modulated structure produced from planar boundaries displaying large displacements (Watanabe, 1979). Below 385°C the CuAu alloy forms in a well-ordered face-centered tetragonal structure. However, between 385° and 410°C the Cu and Au atoms order to produce CuAu II. The size differences of Cu and Au produce structural strain, which is relieved by a more or less regular alternation of Cu and Au on the several
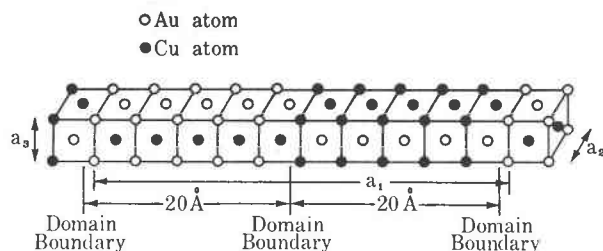
Fig. 1. Sketch of atom positions in CuAu II. This structure is disordered at high temperatures, but orders and thereby forms out-of-phase domains and positional modulations on cooling. (From Watanabe, 1979)

structural sites (Fig. 1). Out-of-phase boundaries separate regions where Cu is on one set of the face centers from regions where Au occupies these sites. The boundaries have, on the average, spacings that are about five times that of the sub-cell, and they can readily be imaged by electron microscopy at low to moderate magnifications (Fig. 2). The average periodicity varies with the Cu-Au ratio and with the addition of other elements in small quantities.

Antigorite, a serpentine mineral with composition $Mg_{3-x}Si_2O_5(OH)_{4-2x}$, is an example of a silicate in which a small structural misfit results in modulations. The difference in dimensions of the octahedral hydroxide sheet and adjacent tetrahedral silicate sheet produces a structure having a corrugated appearance (Fig. 3). These sinusoidally distorted regions commonly have widths greater than ~40Å before they reverse orientations (Kunze, 1956); they are also readily imaged by electron microscopy (Yada, 1979). Figure 4 shows an image of planar serpentine (lizardite) that is intergrown with poorly modulated serpentine. In Figure 5 the antigorite modulations are better developed and more continuous; in this sample the serpentine occurs as an alteration product of pyroxene.

Pyrrhotite ($Fe_{1-x}S$) is a widespread non-stoichiometric sulfide. It typically displays satellite spots having non-integral spacings in its diffraction patterns; their origin and interpretation has been the subject of controversy. However, high-resolution microscopy has indicated details of some of the structural complexities of the several non-integral varieties (Pierce and Buseck, 1974, 1976; Nakazawa, Morimoto and Watanabe, 1976; Morimoto, 1978). Imaging with dark-field (DF) techniques first indicated the existence of anti-phase domains of varied dimensions that alternate paral-
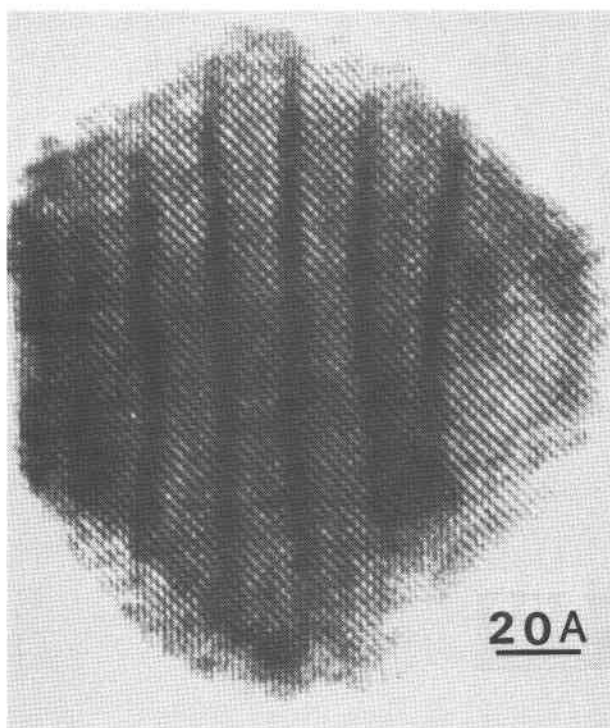

Fig. 2. Image of a small crystal of CuAu II, showing modulations with spacings of ~20Å. (From Mihama, 1971)

lel to c and that result from supercells produced by ordered Fe vacancies. Figure 6 shows such a DF image, with the anti-phase boundaries indicated by arrows. This structure, with an average periodicity along c equal to 5.1 times c, consists of a mixture of domains having dimensions of five and six times the length of c in the pyrrhotite subcell. By analogy, it is clear that a large number and variety of non-integral diffraction patterns and incommensurate modulated structures can occur in pyrrhotite simply from various mixtures of domains having different dimensions.
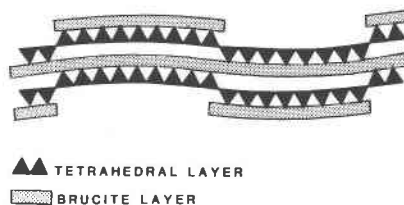

Fig. 3. Sketch of the structure of antigorite serpentine. Strain produced by the dimensional mismatch between the tetrahedral layer (indicated by triangles) and the brucite-like octahedral layer (shaded) results in roughly periodic boundaries and thus structural modulations. The wavelength of the modulation is ~40Å. (Adapted from Kunze, 1956)
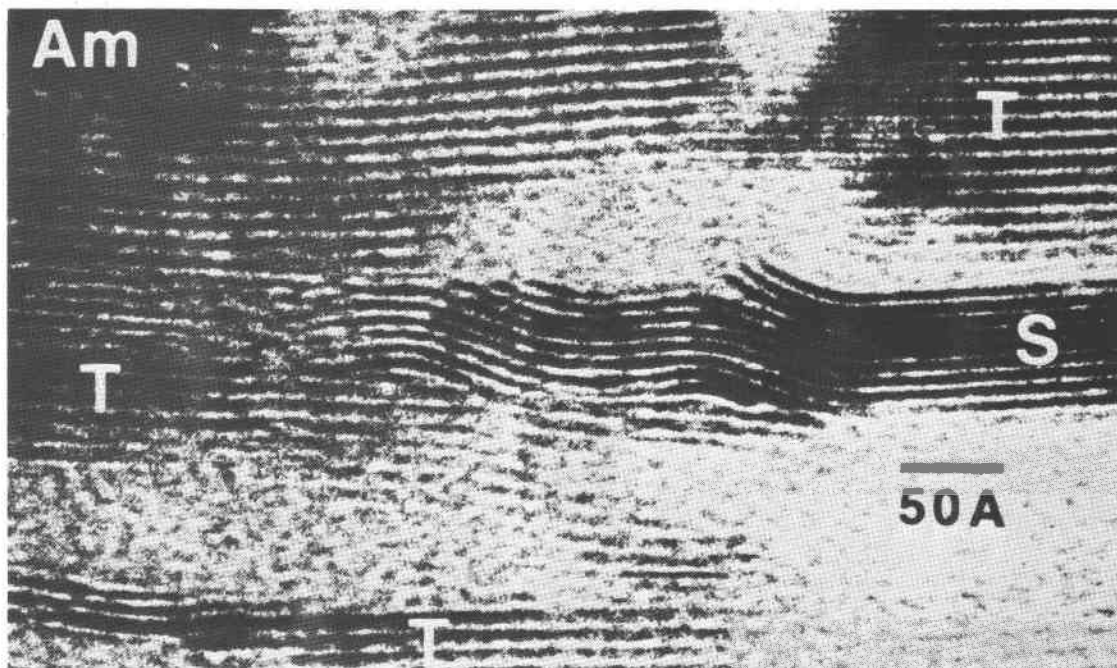
Fig. 4. Image of undulating serpentine structure, continuous with planar serpentine(S) and intergrown with talc(T). The wavelength of these modulations is ~150Å, appreciably greater than is typical of antigorite. Specimen is of a uralite form Romania; remnant amphibole (AM) is shown in the upper left corner. (From Veblen and Buseck, 1981)

Large compositional modulations

Relatively large compositional modulations are a common consequence of spinodal decomposition. Such fluctuations occur in many alloys (*e.g.*, Ni 23% Au) as well as minerals. Sulfides such as those from the bornite (Cu_5FeS_4)–digenite (Cu_9S_5) solid solution series provide good examples of structural variations produced by compositional changes, some of which may be related to spinodal behavior. Morimoto and colleagues determined that there exists a series of structures that contain an alternation of regions having all metal sites occupied with regions having clustered vacancies on the cation sites (Morimoto, 1964; Morimoto and Kullerud, 1966; Koto and Morimoto, 1975), and Putnis and Grace (1976) showed electron diffraction patterns of some of the intermediate, transitional stages.

Figure 7 shows an image of digenite (with an unknown but presumably small Cu content) displaying a structural distortion that results in modulations that are observable in two directions. The origin of the fluctuations is presumably a separation into extended vacancy-rich and vacancy-poor regions (Pierce and Buseck, 1978). The structural distortions produced by such vacancy clustering are readily observed by high-resolution imaging.

Sulfides and sulfosalts provide other examples of chemical fluctuations that result in structural modulations. They are well reviewed by Wuensch (1979), and additional examples are given by Makovicky and Hyde (1979). In their study of phases with compositions between chalcocite (Cu_2S) and bismuthinite (Bi_2S_3), Tomeoka and Ohmasa (1982) discovered three such materials. Figure 8 shows an image of a quenched crystal of $Cu_3Bi_5S_9$ that contains domains that are alternately depleted and enriched in Cu relative to Bi. The resulting modulations show up clearly in TEM images, where the spacings between corresponding layers average roughly 18Å (Tomeoka *et al.*, 1981).

Modulations are common in TEM images of carbonates such as calcite and dolomite (*e.g.*, Reeder, 1981; Reeder and Wenk, 1979), but the origin of the modulations is not clear. Gunderson and Wenk (1981) have described long-period modulations in low-Mg calcite and suggest the modulations formed during an ordering phase transformation, although further confirmatory work is indicated. Reeder and Nakajima (1982) find that cation ordering in dolomite occurs via a twinning mechanism. It appears as if dolomite and magnesian calcite provide good examples of minerals that display modulations that are, as yet, not completely understood.
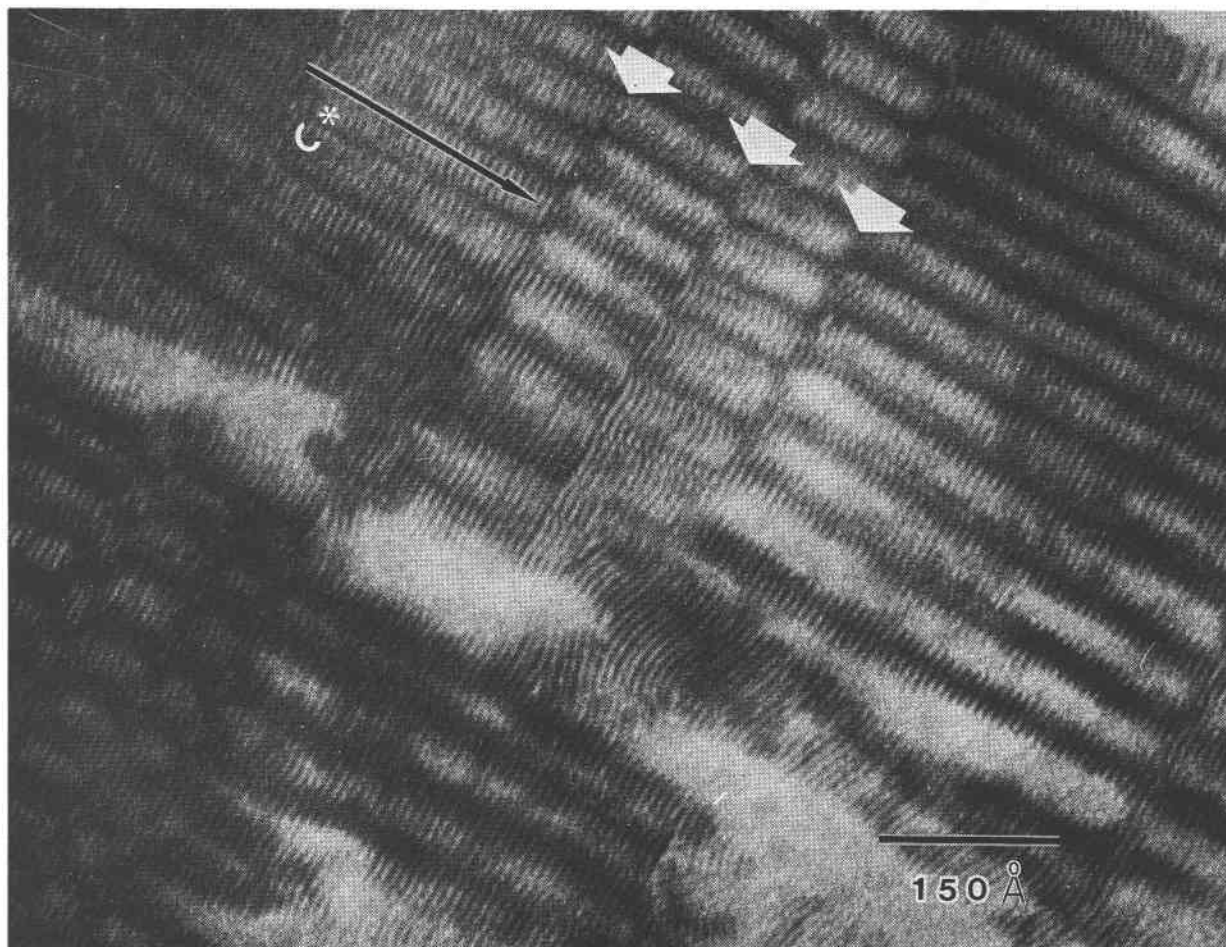
Fig. 5. Image of regularly modulated antigorite, with a wavelength that ranges between 45 and 50Å. The modulations appear as the dark bands perpendicular to c^*. Out-of-phase or twin boundaries are also present and are indicated by the white arrows. Specimen is from a bastite from the Jeffrey Mine in Quebec. (From Spinnler *et al.*, 1982)

Crystallographic shear (CS) planes give rise to homologous sets of structures in many simple chemical systems, and especially in oxides of metals having variable oxidation states. Such CS planes in TiO_2 and WO_3, and the numerous compositions and structures derived from them by reduction, have been imaged in a series of electron microscopic studies. A good review of some of the structures and papers about them is provided by Hyde (1979). Iijima (1975) has shown the nucleation and growth of individual CS planes in WO_{3-x} (Fig. 9) and how they then combine to form a regularly ordered, modulated, long-period structure. A large family of phases related to slightly oxygen-deficient rutile occurs, again resulting in long-period structures of great variety and varied complexity (*e.g.*, Grey and Bursill, 1978; Hyde, 1976 and references therein).

Periodic compositional changes and small displacements

Feldspars exhibit disordered Al–Si distributions at high temperatures, but on cooling these elements order. In the process, lattice strain is developed and it, in turn, tends to stabilize structures to temperatures lower than they would exist in the absence of such strain (Goldsmith and Laves, 1954; McConnell, 1971). Such metastable persistence commonly results in modulated structures, characterized by small atomic displacements from their idealized, strain-free configurations. Aspects of the electron microscope observations of such modulations are given by Morimoto (1979), Miúra (1979), and Wenk and Nakajima (1979). Horst *et al.* (1981) provide details of modulations for a labradorite plagioclase, together with an extensive lit-
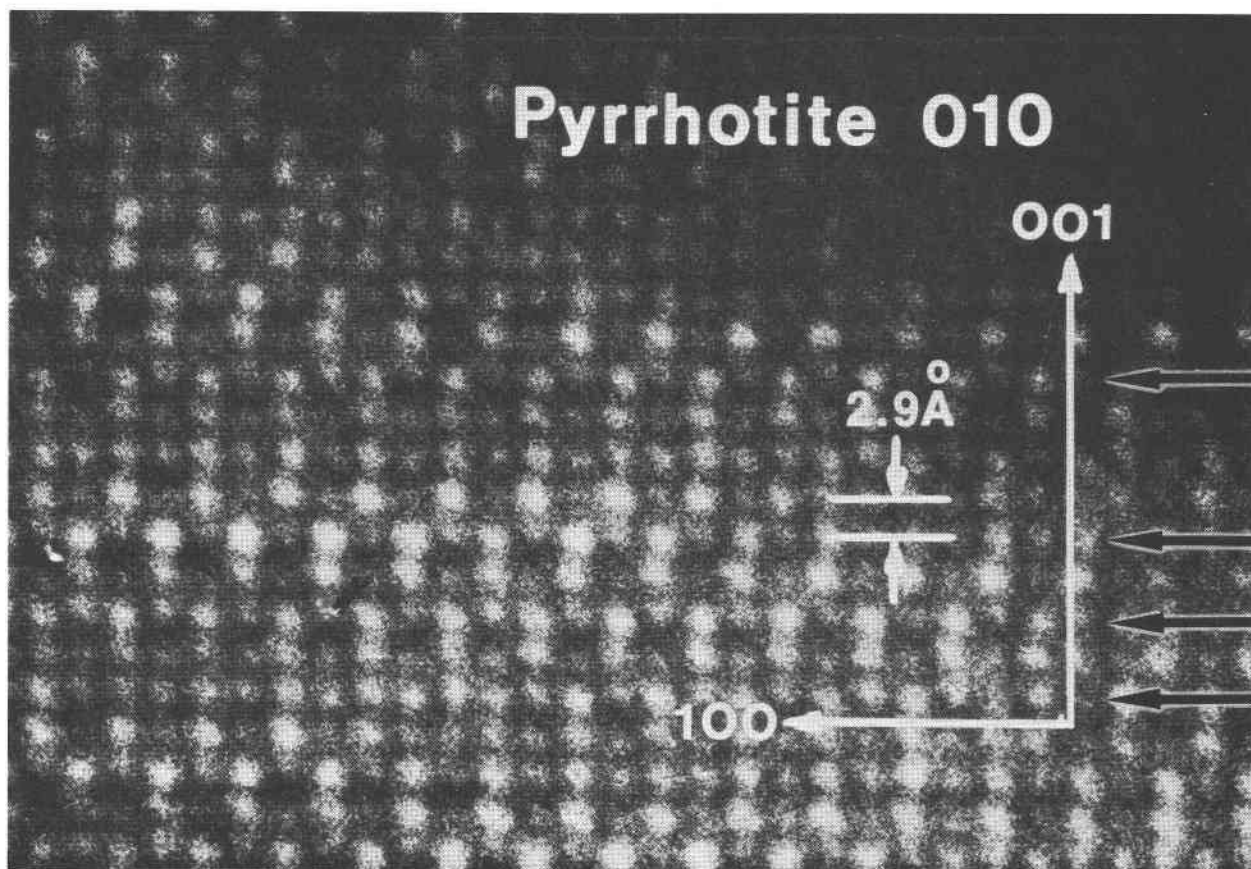
Fig. 6. High-resolution dark-field image of pyrrhotite displaying an incommensurate structure. The bright spots are in the positions of columns of Fe atoms, and the corresponding darker regions occur at sites containing vacancies. The vacancies are ordered into layers to produce domains of different c-dimensions (separated by anti-phase boundaries) that result in an incommensurate diffraction pattern (Figure 16). (After Pierce and Buseck, 1974)

erature review, and Smith (1974) has summarized the problem of structural modulations and other complexities in feldspars in general.

The inversion from orthoclase to microcline is accompanied by ordering and consequent lattice strain. Eggleton and Buseck (1980) used high-resolution imaging to follow this transition. They found that a sinusoidal fluctuation (Fig. 10) occurs as microcline is produced, but prior to the development of the well-defined twinning that characterizes unstrained maximum microcline. The spacing of the modulation in this sample is $\sim 50 \text{Å}$ parallel to [020], roughly eight times the value of d_{020} and equal to the width of the twin domains in unstrained maximum microcline.

Morimoto (1978), in a review of incommensurate structures, provides a discussion and TEM images of several silicates with incommensurate structures. He provides illustrations of e-plagioclase, mullite, and hauyne, a calcic member of the soda-

lite group. In all cases, he reports that the modulations result from antiphase domains that are distributed statistically in their host structures. Changes in their periodicity and orientation produce the non-integral spacings in diffraction patterns and the changes in positions of the satellite spots.

There is a wide range of compounds having the hollandite structure, reviewed by Post *et al.* (1982), and their large channels permit considerable chemical variability that commonly results in modulations. Bursill and Grzinic (1980) have used electron microscopy to detail the incommensurate modulations that occur in some synthetic phases having the hollandite structure; these modulations result from partial ordering of cations in the channels. Turner and Buseck (in prep.) have observed and described similar effects in natural hollandites as well as in other related Mn oxides.
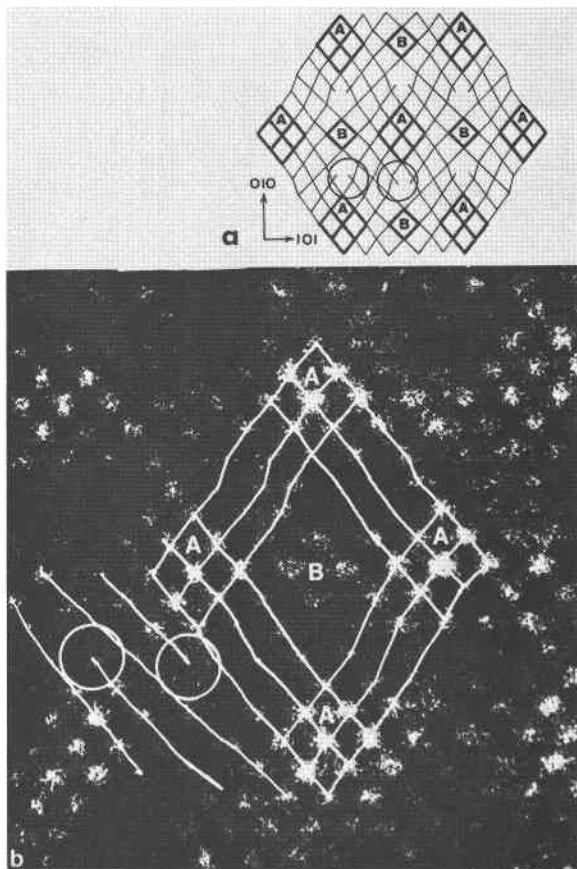
Tungsten bronzes are a family of compounds that

Fig. 7. High-resolution dark-field image of digenite, showing modulations that presumably result from spinodal decomposition. (a) shows an idealized representation of the structure, corresponding to the image in (b). Vacancy clustering has resulted in the formation of two distinct structures (A and B). The circled regions contain discontinuous rows of spots (edge dislocations). The image is ~60Å wide. (From Pierce and Buseck, 1978)

display a range of stoichiometries and defect structures that give them interesting electrical and chemical properties. Their general formula is A_xWO_3, where A represents a large cation, generally of an alkali element, that is situated within large channels that run through the octahedral framework of the structure (Fig. 11) (Magnéli, 1953). In compounds such as $K_{0.3}WO_3$ there are insufficient alkali atoms to occupy all of the available sites, and a structure containing ordered vacancies and thus supercells of different sizes results. Figure 12 shows an image of an incommensurate superstructure with modulations having spacings of 2.2 times c ($c = 7.54$Å), where each subcell contains two alkali sites in the c direction of the subcell (Bando and Iijima, 1980) and every fourth or fifth alkali site is unoccupied. The non-integral periodicity is a consequence of the mixing of domains having distinct c-dimensions. In this sense the incommensurate character is related to that shown by pyrrhotite and $Cu_3Bi_5S_9$, described above.

Intergrowth of structures with different symmetries or compositions

There are numerous examples where distinct but related structures are intergrown coherently. In many cases such intergrowths occur randomly, but in some crystals long-range periodicities develop. Such crystals commonly display integral spacings, although incommensurate ones clearly can also occur. An example is if the two (or more) structures are intergrown in a sequence that is periodic only in a statistical sense, *i.e.*, on average the intergrowths have a certain fixed wavelength. Whether or not the intergrowths result in commensurate or incommensurate spacings, the large repeat distances, combined with two or more types of subcells that represent the substructures, commonly result in characteristics similar to those of modulated structures. There are many possible examples, but we shall select two—the synthetic alkali tungsten bronzes and some of the biopyribole minerals—to illustrate the images of these types of materials.

Some characteristics of tungsten bronzes (TB's) were described in the previous section. They can occur with either tetragonal or hexagonal symmetries (TTB or HTB, respectively), and they can intergrow with alkali-free WO_3. Kihlborg and his colleagues (*e.g.*, Sharma and Kihlborg, 1981) have synthesized a variety of compounds by substituting Ta, Nb, or V for the W as well as by introducing different alkali ions within the channels. The resulting structures display a fascinating variety of ordered and disordered intergrowth types. Some ordered structures have repeat periods greater than 150 Å. An example of what the authors have called intergrowth tungsten bronzes (ITB) is shown in Figure 13. The authors speculate on the origins of these complicated ordering sequences, but their origin is not understood. Sharma and Kihlborg (1981) point out that investigation of these structures would have been impossible without HRTEM.

The biopyriboles and related sheet silicate minerals display a variety of intergrowth structures and in these, too, HRTEM has been critical for clarifying the intergrowth details (Veblen and Buseck, 1979a,b,c). There are a variety of chain silicates in which slabs containing chains of different widths can intergrow coherently. When all of the chains
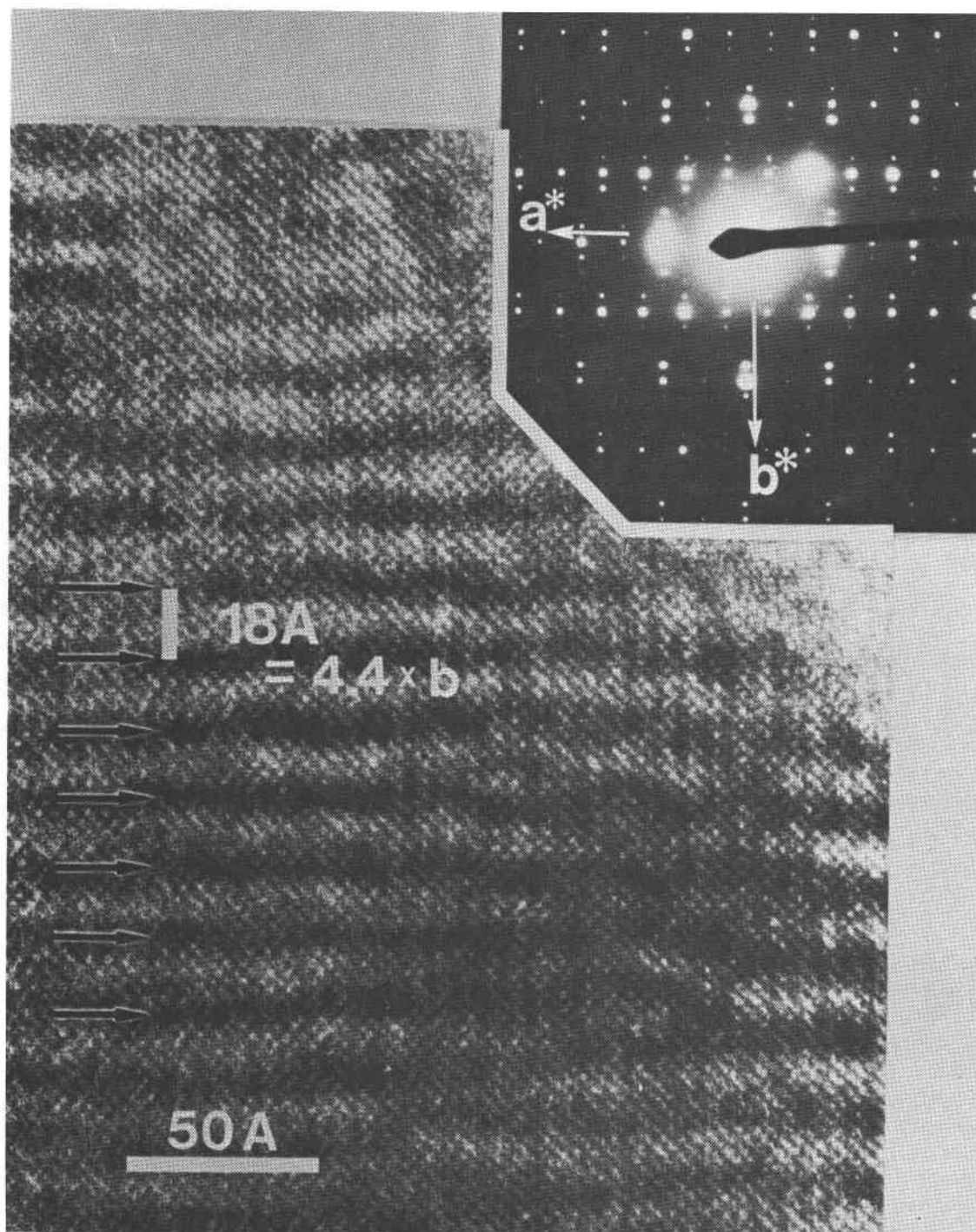
Fig. 8. Image of $Cu_3Bi_5S_9$ showing modulations in intensity running parallel to b. Ordering of Cu and Bi results in an incommensurate modulated structure having a wavelength that is 18Å, roughly 4.4 times the b dimension. The inset shows the corresponding electron diffraction pattern, with the 18Å satellite spots arrayed parallel to b^*. (From Tomeoka *et al*, 1981)

are of equal widths, or in ordered sequences, they give rise to well-known minerals such as pyroxenes, amphiboles, jimthomsonite, and chesterite. They also occur in disordered arrays, as well as in long-

period regular sequences that do not correspond to any minerals known to occur on a macroscopic scale. These sequences (Table 2) have a low probability of occurring by random processes (as low as
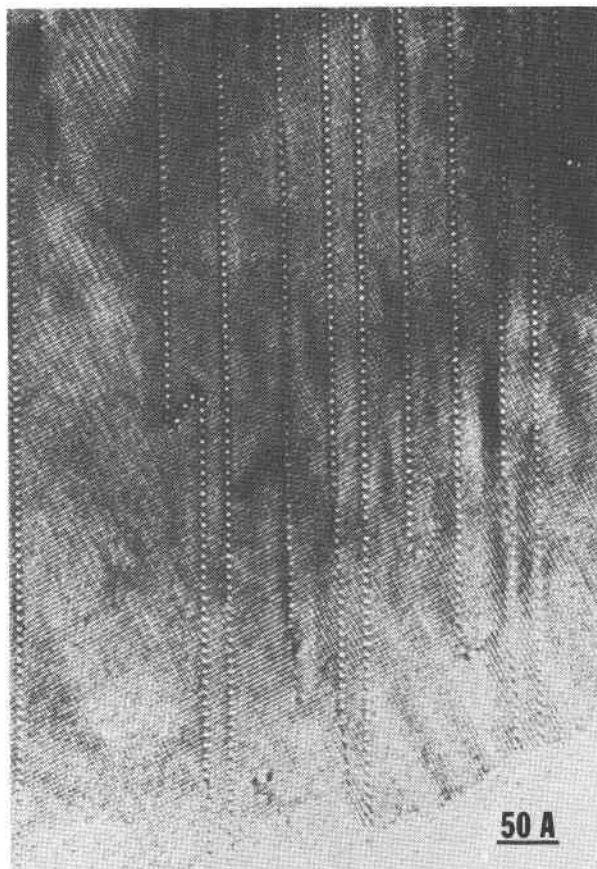
Fig. 9. High-resolution image of WO_{3-x}, showing the incipient formation of a modulated structure. Reduction of WO_3 results in the formation of CS planes (linear features containing white spots) which, with increased reduction and annealing, would result in well-developed modulations. (From Iijima, 1975)

10^{-45} for 2333, illustrated in Figure 14), although there is insufficient evidence to determine whether they result from special growth processes or as a result of their thermodynamic properties. They bear a distinct similarity to the synthetic long-period sequences of ITB that are described above. The modulations of the biopyriboles and ITB's that have been observed to date are commensurate, although their characteristics would appear to allow the occurrence of non-integral intergrowths if, for example, chains having different widths or slabs with different substructures were intergrown in a semi-regular fashion.

HRTEM methods have also allowed the imaging of intergrowths of different types of layer silicates. Figure 15 shows intercalated chlorite, talc, and lizardite serpentine as one example; many others also occur, especially with clay minerals. The layer silicates can readily crystallize into coherently in-

tergrown crystals containing structural elements of different types; they are thus prime candidates for the development of regular, long-period intergrowth structures and for incommensurate behavior.

Electron diffraction and microdiffraction

While high-resolution imaging is well suited for observing the localized structural details of modulated crystals, it is commonly necessary to use electron diffraction patterns as the primary sources of information. This situation obtains where high-resolution imaging is not possible, as in the case of crystals that suffer rapid electron radiation damage and where larger regions of crystals are to be studied than can be examined conveniently by direct imaging. Also, diffraction results allow ready determination of average periodicities that may not be clear in an image.

Electron diffraction provides an immediate impression of features that can be observed only with careful experimentation and long exposures with X-ray diffraction. Patterns visible on a fluorescent screen or recorded on film in a few seconds can show weak extra diffraction spots, lines, bands, arcs, and other diffuse scattering. The geometry of the diffraction effects is clear because with the very short wavelength normally used (0.037Å for 100 keV electrons) the Ewald sphere has a very large radius and the pattern represents an almost planar section of reciprocal space. The result is a wealth of data. Unfortunately, this benefit is commonly offset by the fact that strong dynamical diffraction effects can make the data difficult to evaluate.

Electron diffraction patterns are typically obtained by using either a nearly parallel beam of electrons or by increasing the strength of a pre-specimen lens to produce a strongly convergent beam. The former method, called selected area electron diffraction (SAED), can produce structural data from regions 0.5 to 1 μm in diameter when a suitably small aperture is placed into the electron beam. Convergent beam electron diffraction (CBED) yields data from smaller regions and, if the regions have diameters less than 0.1 μm, is commonly called microdiffraction. CBED patterns can provide information of a different sort than SAED patterns, and therefore they are discussed separately.

Selected area electron diffraction (SAED)

Electron diffraction spots from both commensurate and incommensurate structures are clearly evident in SAED patterns. An example of such a
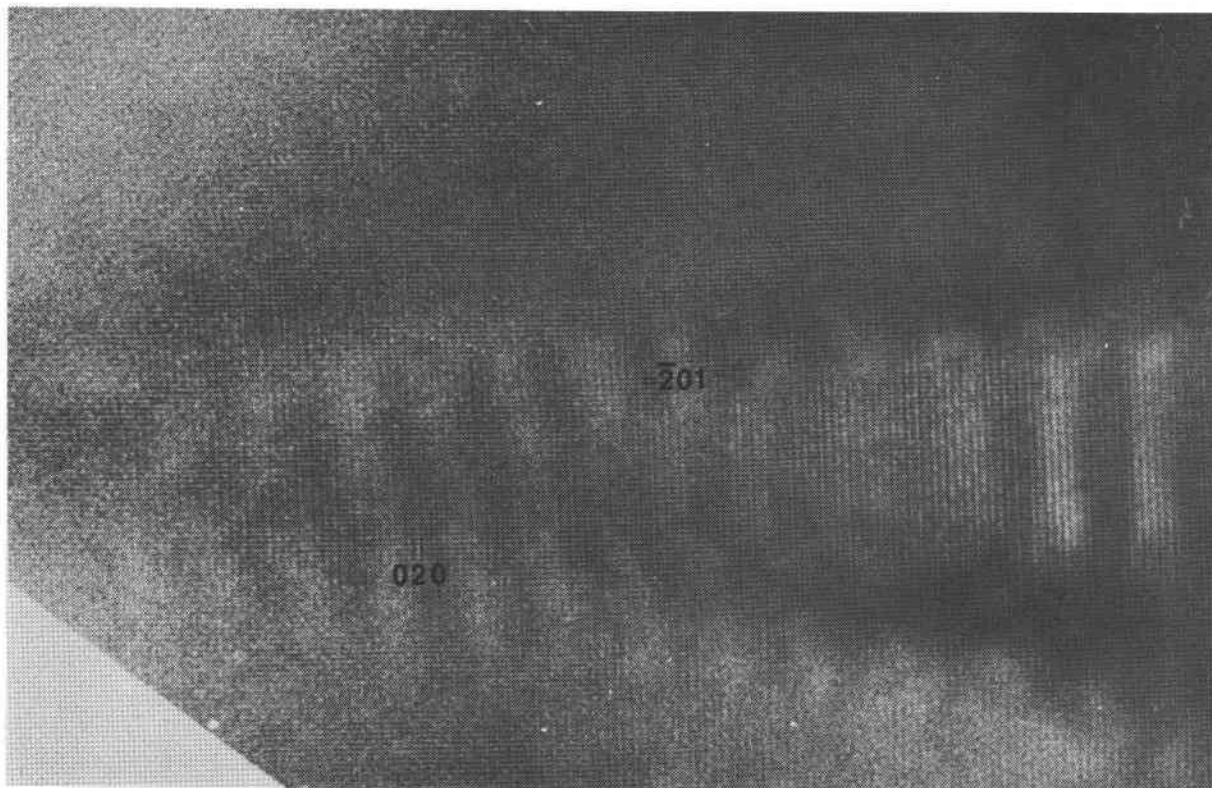
Fig. 10. Image of modulations in feldspar that has transformed incompletely from orthoclase to microcline. The sinusoidal fluctuations result from Al-Si ordering and can be observed by sighting along [020]. $d_{\bar{2}01} = 4.2\text{Å}$. (From Eggleton and Buseck, 1980)

pattern from pyrrhotite is shown in Figure 16, where the strong reflections from the well-ordered substructure are sharp and clear. The weaker spots arising from the superstructure show a well defined incommensurate periodicity. An HRTEM image from a similar crystal (Fig. 6) shows that this periodicity represents an average over domains having dimensions several times the c-axis of the pyrrhotite subcell. There are weak continuous streaks between the superstructure spots, indicating that the ordering of the superstructure is imperfect.

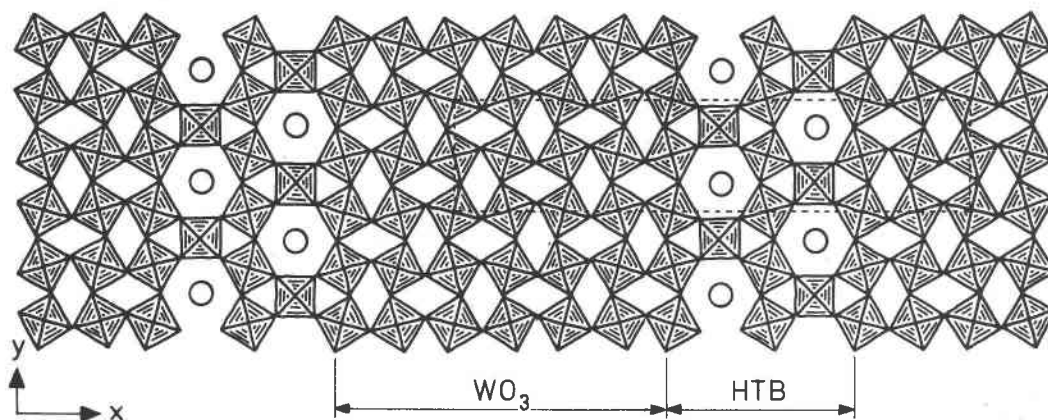The SAED pattern usually represents an average

Fig. 11. Schematic diagram of an intergrowth of the hexagonal tungsten bronze (HTB) and the WO_3 structures. The WO_6 octahedra are joined by corner-sharing. Alkali atoms (large circles) can fit into the large channels in the HTB. (From Sharma and Kihlborg, 1981).
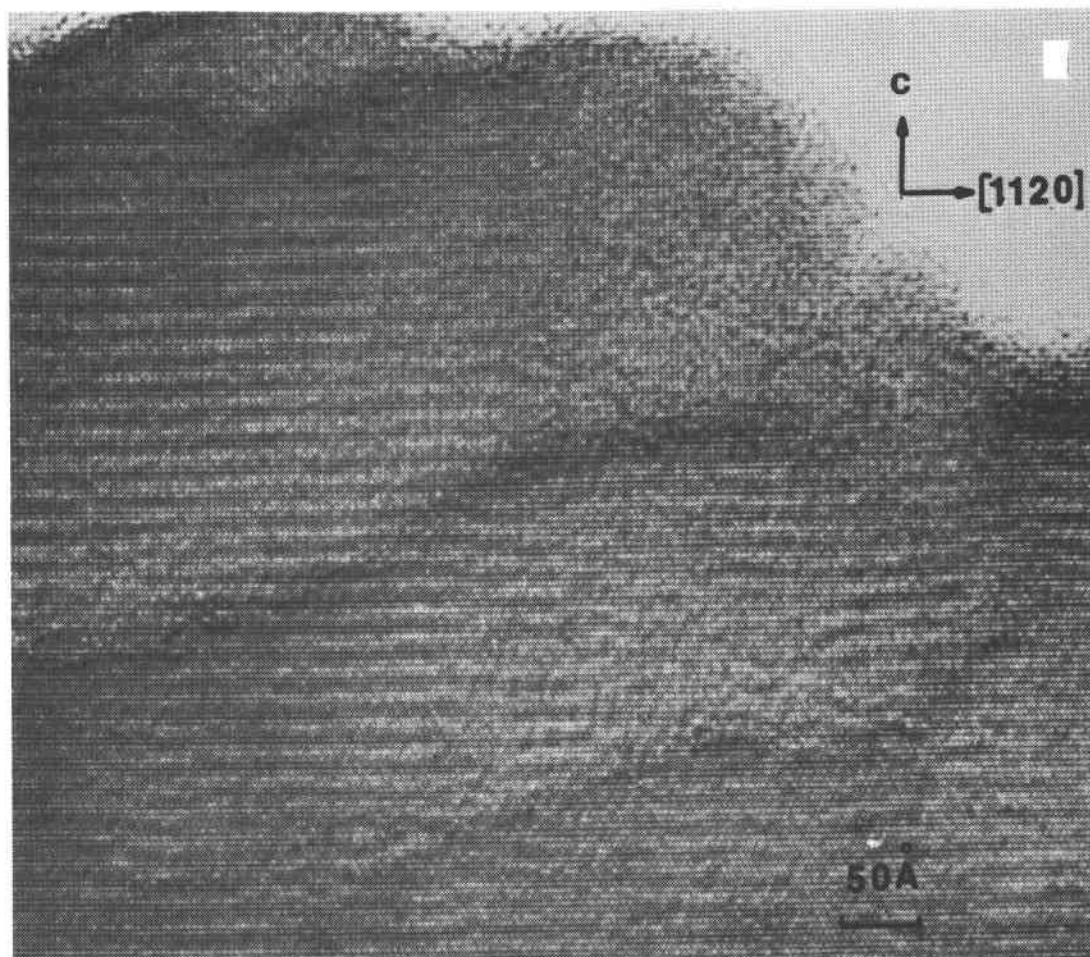
Fig. 12. High-resolution image of incommensurate modulations in HTB. The channel occupancies (*cf.* Figure 11) are incomplete, resulting in domains of different widths. Note that the modulations are well displayed in the thicker portions of the crystal. (Bando and Iijima, 1980; photograph from Iijima)

over an area roughly at least ten times as great as that shown in an HRTEM image. It is unusual for crystals to have small and uniform thicknesses over regions 1 μm or so in diameter. Thus, SAED patterns usually represent an average over a large range of thicknesses and tend to be dominated by the contributions from the stronger-scattering thicker parts. For these regions the dynamical effects may greatly affect the intensities, increasing the intensities of very weak reflections so that they are relatively strong.

An extreme case of the effects of dynamical scattering in relatively thick regions of crystal is illustrated in Figure 17. The 200 reflection of silicon is forbidden by the kinematical symmetry extinction rules and so has no appreciable intensity for very thin crystals. The results of calculations by Tu and Howie (1978) show that this is so for the first 100 to 150 Å of thickness, during which the allowed 111 reflection has increased to a maximum value and then decreased again. However, for thicknesses greater than about 150Å the 200 reflection increases rapidly in intensity to become comparable with the other, kinematically allowed, reflections. The presence of the 200 reflection has an important influence on the appearance of ultra-high resolution images of silicon, determining the apparent separation of the image spots that correspond to the closely spaced rows of atoms seen in the [110] direction (Hutchison *et al.*, 1982).

Enhancement similar to that described for silicon is possible for the weak reflections arising from long-period structural modulations. Thus, dynamical effects can make it easier to detect structural modulations. On the other hand, dynamical effects also can suppress particular types of diffuse scatter-
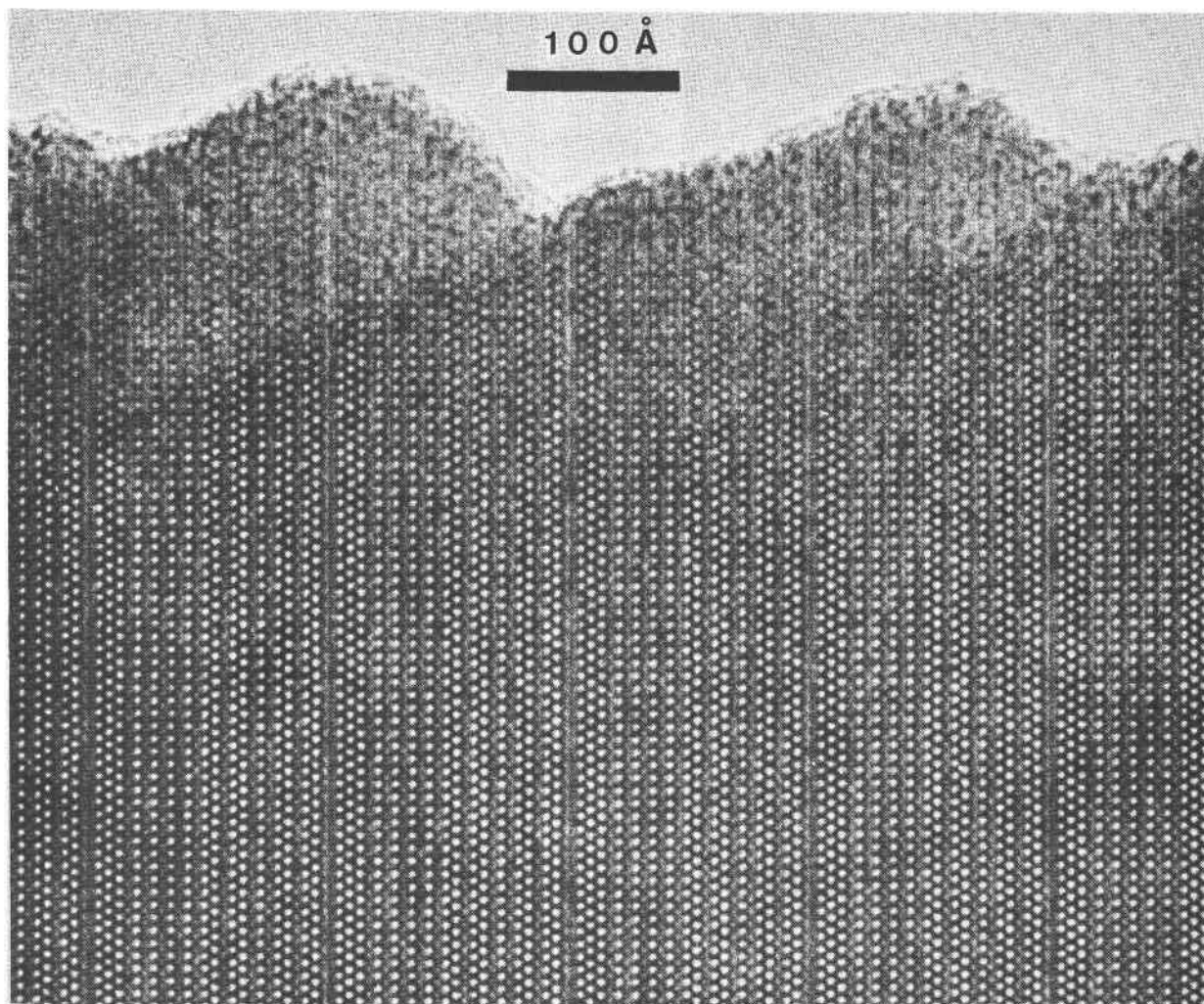
Fig. 13. High-resolution image of intergrowth tungsten bronze of composition $Cs_{0.8}(Nb,W)O_3$. The two regions of structure correspond to HTB and WO_3 (*cf*. Figure 11), intergrown to give a repeat distance of 143Å. (Sharma and Kihlborg, 1981; photograph from Kihlborg)

ing or weak reflections such as those resulting from small atom displacements (including thermal diffuse scattering). In general, the presence of dynamical scattering makes it difficult to interpret electron diffraction intensities. Nonetheless, with the recent advances in the understanding of dynamical diffraction processes, it is commonly possible to make useful deductions.

It is convenient to consider first a thin crystal, where only kinematical effects are important. Figure 18 shows a sketch of a row of diffraction spots from each of two crystals having modulated structures. Distance across the diffraction patterns is plotted horizontally and intensity is plotted vertically. The direct beam is in the center of the horizontal axis and is marked "0".

Figure 18a shows the diffracted intensity for a crystal where the modulations arise from small atom displacements. Note that in this case the satellite peaks around the direct beam have minimal intensity. The maximum satellite intensities occur at some distance from the direct beam, about $2Å^{-1}$, that is determined by the sizes of the atoms. The intensities of the satellite spots tend to be symmetrical around those from the subcell.

Figure 18b is for a crystal in which the modulations arise from atomic ordering, but without displacement of the atoms from their ideal site locations. In this instance, the satellite peaks close to the direct beam contain appreciable intensity; these peaks decrease in intensity with their distance from the direct beam, in much the same way as the

Table 2. Ordered chain silicates from Chester, Vermont (Veblen and Buseck, 1979b)

Chain Sequence	Maximum Repeats	Probability p	Structural Formula	Primitive Cell Edge
(2)	Macroscopic	---	$M_7Si_8O_{22}(OH)_2$	9 Å
(3)	Macroscopic	---	$M_5Si_6O_{16}(OH)_2$	13 1/2
(23)	Macroscopic	---	$M_{17}Si_{20}O_{54}(OH)_6$	22 1/2
(2333)	45	1.6×10^{-42}	$M_{37}Si_{44}O_{118}(OH)_{14}$	49 1/2
(43332343332423)	4	5.8×10^{-17}	$M_5Si_6O_{16}(OH)_2$	189
(2233)	15	1.3×10^{-16}	$M_{17}Si_{20}O_{54}(OH)_6$	45
(433323)	5	1.9×10^{-8}	$M_5Si_6O_{16}(OH)_2$	81
(233)	11	3.3×10^{-8}	$M_{27}Si_{32}O_{86}(OH)_{10}$	36
(232233)	4	2.1×10^{-5}	$M_{17}Si_{20}O_{54}(OH)_6$	67 1/2
(2234)	4	5.4×10^{-5}	$M_{37}Si_{44}O_{118}(OH)_{14}$	49 1/2
(2332323)	3	3.3×10^{-4}	$M_{61}Si_{72}O_{194}(OH)_{22}$	81

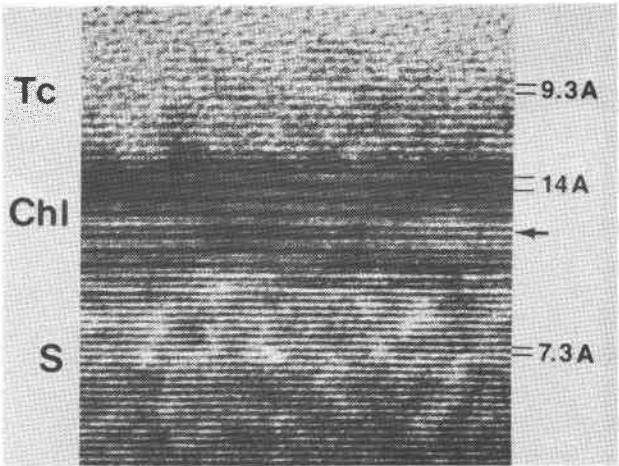$M = Mg, Fe^{2+}, Ca, Mn^{2+}$

Fig. 15. Image of coherently intergrown chlorite (Chl), talc (Tc), and lizardite serpentine (S). The arrow points to an extra layer of talc within the chlorite. (From Buseck and Veblen, 1981)
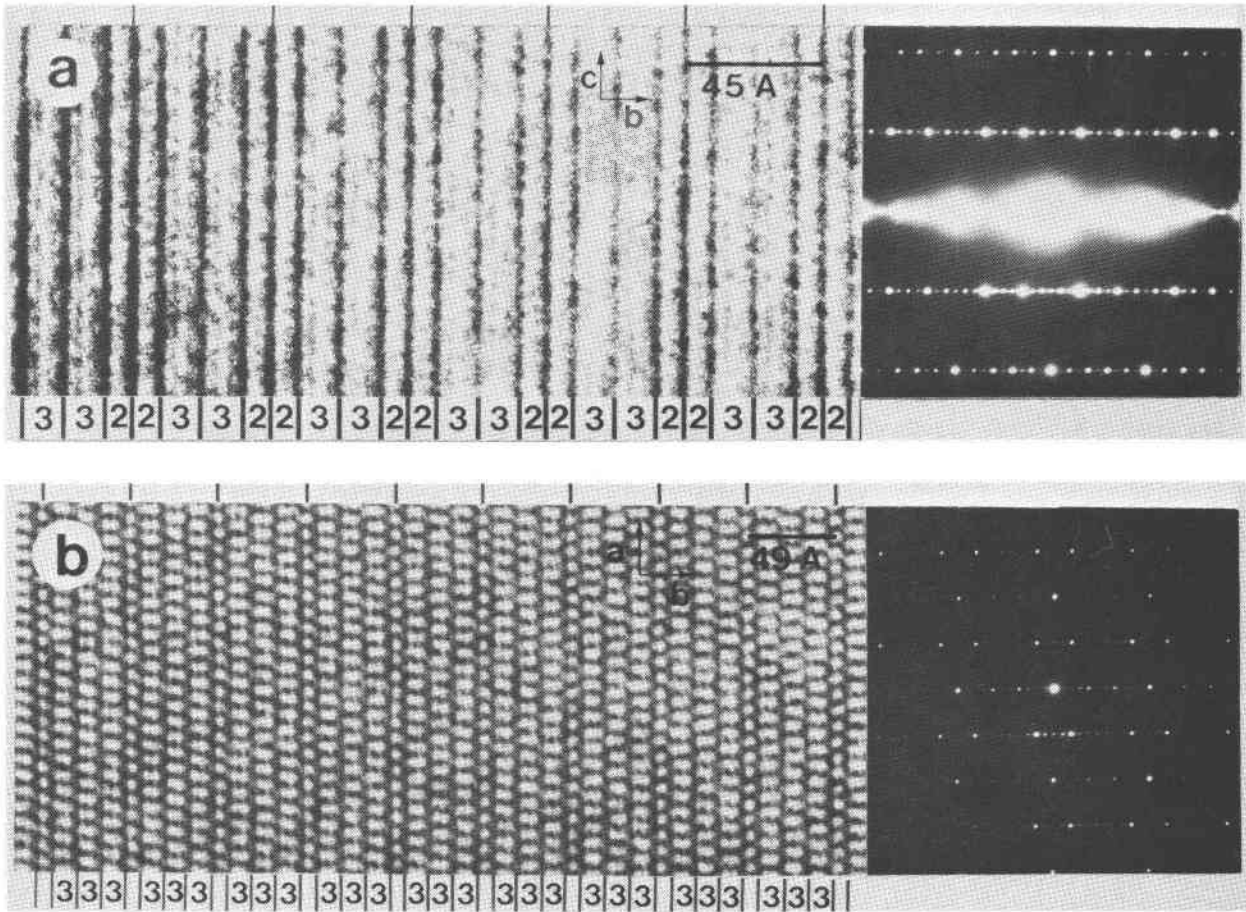

Fig. 14. High-resolution image of chain silicates having long repeat periods. The ordering sequences are 2233 (top) and 2333 (bottom), where a "2" signifies a double silicate chain and a "3" a triple chain. The double-chain slabs are unlabeled in the lower image. Unit-cell spacings are indicated by marks above the images and equal 45 and 49 ½Å respectively. (From Veblen and Buseck, 1979a)
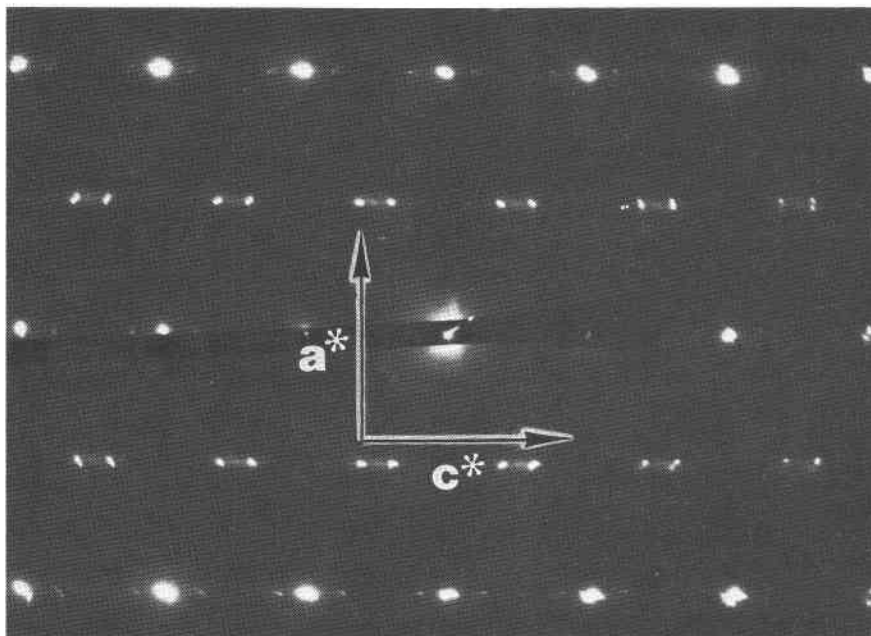
Fig. 16. SAED pattern of pyrrhotite showing non-integral spacings of the weaker satellite diffraction spots and also streaking between these spots, indicating some disorder in the long period modulation. (From Pierce, 1979)

substructure spots and in marked distinction to the satellites resulting from atom displacements. Many real crystals of course contain both atomic ordering and small displacements and so display diffraction effects that are intermediate between those in Figures 18a and b.

Proper interpretation of diffracted intensities is more complex for crystals that are thick enough to produce strong dynamical scattering (and that is the most common case). It has been shown (Cowley and Fields, 1979) that for many cases the effect of the dynamical diffraction can be well approximated by multiplying the intensity distribution in the diffraction pattern, calculated using kinematical theory, by a "dynamical factor." This factor is a slowly varying function of position in the pattern; it has a form that depends on the nature of the deviation from the average structure. An example is shown in Figure 19. In theory, the substructure peaks should still be useful for distinguishing between atom displacements and ordering, but the effects are far more subtle than for thin crystals. In general, however, the fact that the dynamical factors are slowly varying functions means that the relative intensities of small groups of satellite spots are not strongly affected. Hence the information on the periodicities and general character of the modu-

lation, on a scale that is larger than that of the substructure, is recoverable. These conclusions have recently been verified by calculation of diffraction intensities of superlattice reflections and the corresponding high-resolution images for heavy-atom alloys (Shindo, 1982).

In principle, detailed calculations of dynamical effects on diffraction intensities is possible, and these intensities should be very sensitive to the fine details of the structure and its modulations. However, the experimental and computational techniques are not yet refined to the stage where it is possible to take full advantage of this situation.

Finally, we should mention that in SAED patterns it is common to see streaking of those spots that arise from the long-period modulations, as is the case in Figure 16. This is an indication that there is some disorder or faulting in the sequence of repeat units. Such irregularities are not surprising; the energy terms that induce the long-range periodicity are usually relatively small, so that mistakes in the ordering are not unusual.

Convergent beam electron diffraction (CBED)

While SAED patterns are useful for studying many aspects of modulated structures, CBED patterns can provide different types of information. Structural
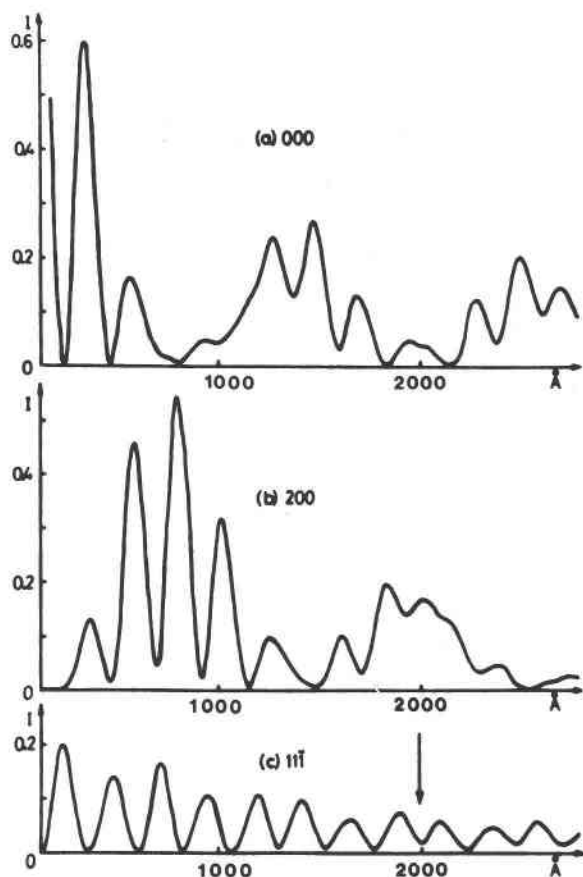
Fig. 17. Calculated plot of intensity *vs.* crystal thickness for the direct beam, 000, and the 200 and 11Ī diffracted beams in silicon. Although 200 is forbidden and has almost zero intensity for thicknesses less than about 150Å, the intensity increases with thickness to a maximum around 800Å. (From Tu and Howie, 1978)

Fig. 18. Schematic drawing of diffraction intensities (vertical) *vs.* lattice spacings (horizontal) for kinematical scattering for several orders of reflections from a thin crystal. The position of the direct beam is labeled "0." The distribution of intensities of the satellite peaks varies, depending on whether the modulations result from (a) small atomic displacements or (b) atomic ordering.

Pattern (a) was obtained by selecting the desired area of the specimen in a scanning image and then stopping the beam and immediately recording the patterns by use of a TV camera and videotape so that the pattern was obtained in about 1/30 second. For (b) several videotape frames were integrated to give a less noisy pattern. Pattern (c) is the vague remnant of a pattern recorded after the beam had been stopped at one point for about 1 second.

Fig. 19. Schematic drawing of diffraction intensities *vs.* reciprocal lattice spacings for a crystal that is thick enough for dynamical scattering to be significant. This example is for a crystal in which the modulation results from small atomic displacements (*cf.* Figure 18a). (a) shows the variations in satellite intensities for a thin edge. When multiplied by (b), which is an appropriate "dynamical factor" (Cowley and Fields, 1979), the dynamical intensities in (c) result.

data can be obtained from far smaller areas (down to 5 to 10Å in diameter), space group symmetry information can be determined, and in special cases three-dimensional structural data can be obtained. All of these features have potential applications for the study of modulated structures.

If a strongly convergent electron beam is used, then probes having diameters approaching atomic dimensions can be obtained. These can, in turn, be used to produce CBED patterns from correspondingly small regions. It is, of course, necessary that the crystal to be studied can withstand such a concentration of energy. Figure 20 shows several diffraction patterns obtained from regions about 15Å across in a thin sample of disordered kaolinite. The kaolinite is sensitive to electron irradiation and the patterns disappeared in much less than 1 second.
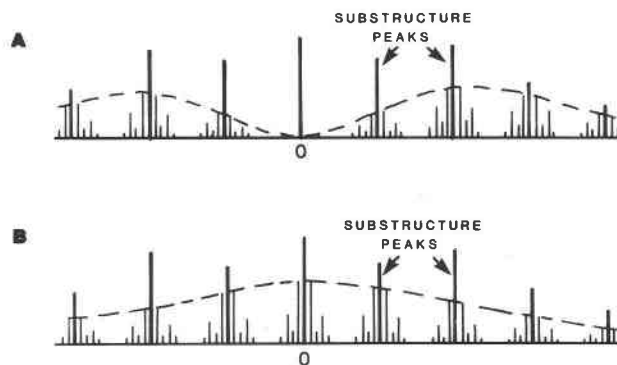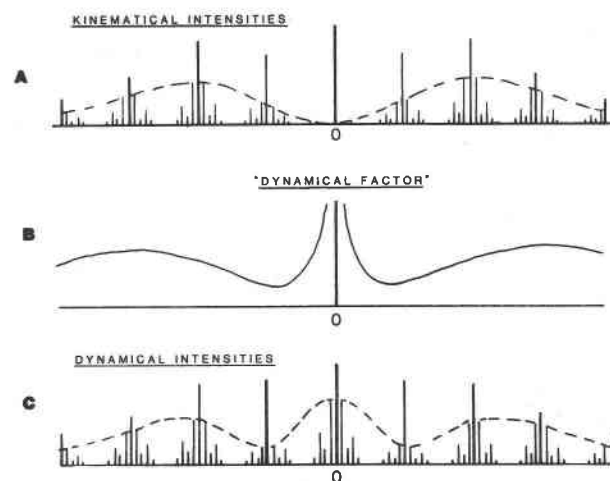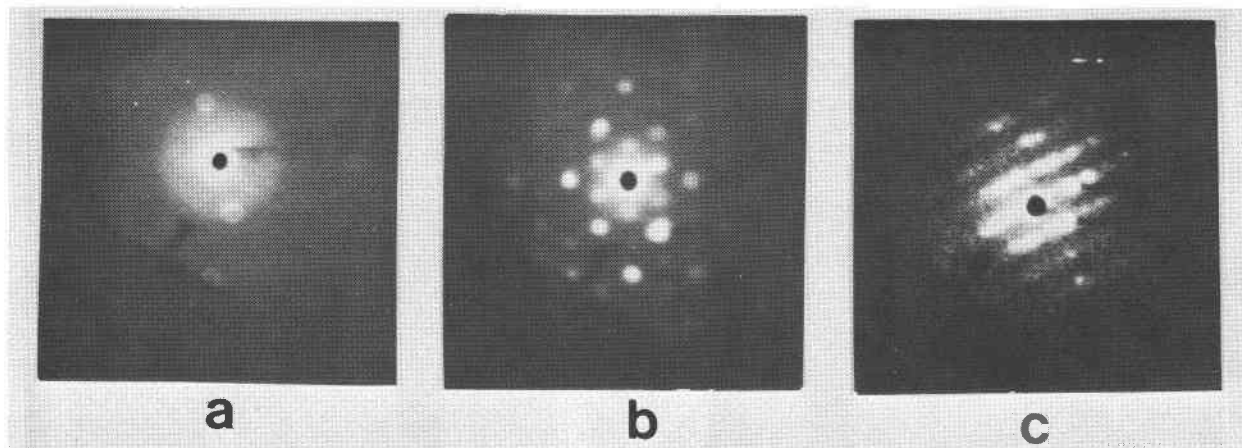
Fig. 20. CBED patterns of kaolinite, using an electron beam with a 15Å diameter. The patterns in (a) and (b) were obtained by exposures of a fraction of a second using an HB-5 dedicated STEM from VG Microscopes Co. For (c) the exposure was about one second and indicates the rapid radiation damage that can occur while obtaining such microdiffraction patterns. (From Cowley, 1981a)

Figure 21 shows a series of CBED patterns of $Ti_2Nb_{10}O_{29}$, obtained with a probe of diameter 10Å as the beam was moved progressively across a single unit cell of the structure which, in this projection, has periodicities $a = 25.8$Å, $c/2 = 10.4$Å. It is evident that the relative intensities of the diffraction beams vary strongly with the position of the probe within the unit cell. While it should be possible to calculate the intensities for such patterns, no practical means has yet been devised for using the observed intensities to derive structural information. The possibility clearly exists, however, of observing the detailed structural changes within the longer dimensions of the repeat units of modulated structures.

Goodman and Lehmpfuhl (1968) demonstrated that a consequence of dynamical scattering, as typically occurs with electron diffraction, is that diffracted intensities are sensitive to the phases of

the relevant structure factors. Therefore, the symmetry of the space group can be determined—even for structures that lack a center of symmetry. Careful study of the symmetry of a CBED pattern, combined with the intensity variations of the extinction bands that occur within the diffraction disks, permits a determination of the projected symmetry of the crystal. A good review is provided by Steeds (1979).

Figure 22 is a CBED pattern of CdS. The positions of the diffraction disks suggest both horizontal and vertical axes of symmetry or mirror planes. However, examination of the extinction bands within the disks shows that reflection symmetry occurs only around the horizontal axis, [000l], but not around any other direction in this projection. Local variations in symmetry within modulated structures can be determined in similar fashion.

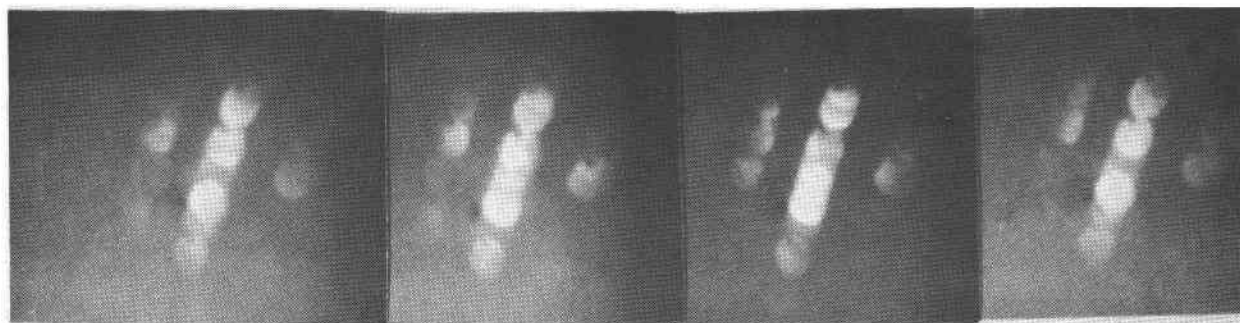A final example of the utility of CBED patterns is

Fig. 21. CBED patterns of $Ti_2Nb_{10}O_{29}$ using an electron beam with a 10Å diameter. These patterns were obtained at four different positions of the beam that all lie within the length of a unit cell; they show that structural variations can be detected and recorded on such a small scale. (From Cowley, 1981b)
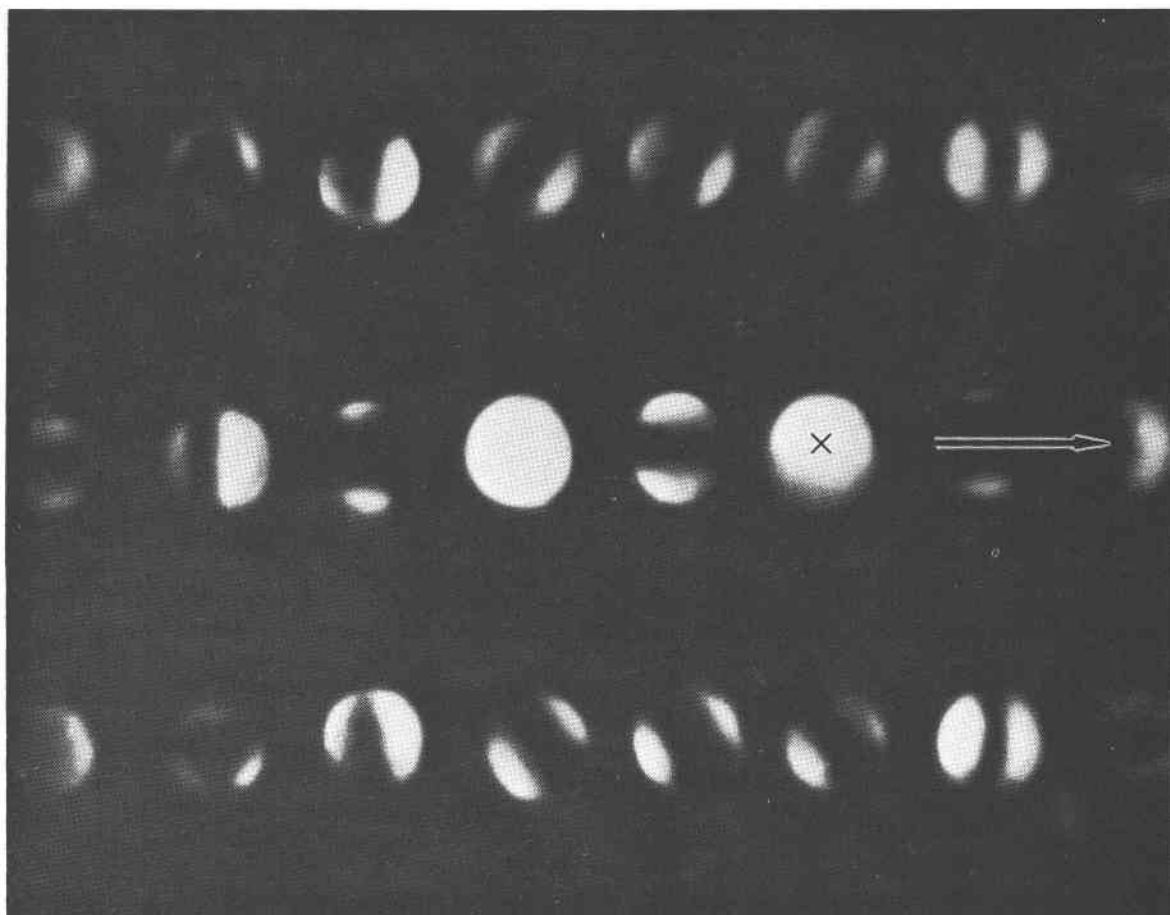
Fig. 22. CBED pattern of synthetic greenockite, CdS, showing symmetry information. In [10$\bar{1}$0] orientation, the CdS has a horizontal reflection plane, but lacks a vertical reflection plane and center of symmetry, and these features are clearly shown by the intensity distributions within the diffraction disks. The arrow is parallel to [0001]. The cross marks the position of 000. (From Goodman and Lehmpfuhl, 1968)

their use to obtain three-dimensional information regarding crystal structure. Normally, any given electron diffraction pattern provides data for only one plane in reciprocal space, the zero order Laue zone. However, by using CBED patterns it is also possible to observe and measure diffraction spots from the *first* and *higher order Laue zones* (FOLZ and HOLZ, respectively). The separation in the diffraction plane between the spots in the zero layer plane and the FOLZ and the HOLZ spots depends on the electron wavelength, the camera constant, and the reciprocal cell dimension in the direction parallel to the electron beam. Since the two instrumental variables can be evaluated, it is possible to determine the cell dimension and thereby obtain a lattice spacing in a direction perpendicular to the primary diffraction plane.

Planar disorder that results in stacking defects parallel to the plane of the zero layer produces smearing of the HOLZ rings (Steeds, 1979) and so can be detected in CBED patterns. For layered minerals such as the layer silicates, modulations that result in polytypism can be detected without the need to orient crystals with their cleavage planes parallel to the electron beam. (Obtaining such orientations can be a severe problem for high-resolution imaging.) However, in order to obtain good CBED patterns for detecting polytypism, it is necessary to use perfect crystal regions 100Å or more in diameter. The direct imaging methods are essential for the study of disordered layer stacking.

The above application of CBED patterns can be applied to many crystallographic problems, modulated structures among them. Liliental *et al.* (1981) used the method to study the structures of pyrrhotite grains that are far too small to examine by single

crystal X-ray methods and even too tiny to obtain good SAED patterns. They describe 3C pyrrhotite, similar to that described by Pierce (1979) from HRTEM imaging, except that their interpretation utilizes measurements of HOLZ lines in CBED patterns.

Microanalysis

The discussion to this point has been largely restricted to the determination of structural effects in modulated structures. However, since modulations can arise from compositional variations, it is clearly appropriate also to consider compositional measurements. In principle, compositional analyses should be possible by either X-ray emission analysis using energy-dispersive spectroscopy (EDS) or by electron energy loss spectroscopy (EELS). The electron probe on a dedicated STEM can be made 5 to 10Å across, which is sufficiently narrow for the resolution and, presumably, analysis of most modulations.

In spite of the theoretical feasibility of direct compositional measurements, there are several experimental limitations that currently restrict the use of microanalysis. All are related to the small volumes of sample that are to be analyzed. A narrow electron probe is required for high spatial resolution, but it results in a poor signal-to-noise ratio and poor counting statistics. Furthermore, except in very thin samples, the beam is spread out over a large diameter by multiple elastic scattering. It is also difficult to determine the precise location of the beam on the sample. At present, it is not generally possible to specify the probe location to better than ~50Å.

Special problems arise with analyses using X-ray emission spectroscopy. The excited volume from which X-rays are produced is significantly larger than all but the very coarsest modulations found in crystals. The excited volume can be reduced by examining very thin crystals, but in this case the counting statistics become extremely poor. The result of these effects is that quantitative microanalysis by EDS on the scale required to determine compositional modulations is not currently feasible. However, in favorable cases it might be possible to observe chemical variations by scanning the electron beam across a compositional interface or modulation, thereby obtaining qualitative data regarding relative changes in composition.

A final problem that can arise when analyzing thin crystals is that electron channelling effects can influence and perturb the intensities (Taftø, 1979). Although such channelling can occur during all microanalyses, the effects are generally negligible for all but very thin crystals.

In summary, microanalysis holds the potential for being useful for the study of compositional modulations. At present, however, the limitations are such that chemical measurements are only useful in special cases, and structural measurements, whether by high-resolution imaging or by electron diffraction, are the methods of choice for studying modulations in crystals.

Conclusion

It is likely that modulated structures are far more common in minerals and synthetic crystals than has generally been appreciated. The streaking and satellite diffraction spots in feldspars have long provided an awareness of their structural complexities, including modulations. Correspondingly close examination of many minerals that have been studied less intensively will likely also reveal periodic or semi-periodic fluctuations.

Electron microscopy is proving to be a major aid for revealing and understanding modulations in crystals. The deviations from perfect periodicity of many modulated structures limit the information that is available from X-ray diffraction measurements. Electron microscopy provides both the necessary spatial resolution and the capability of imaging non-periodic regions to reveal many details of structural fluctuations. Atomic level resolutions are close at hand, and highly localized structural defects can be imaged. Small structural or compositional variations that result in long-period modulations, commensurate or incommensurate, can be revealed. On the other end of the size scale, structural details within unit cells can be measured by both imaging and microdiffraction. Microanalysis using EDS and EELS holds promise for providing at least qualitative information regarding the small compositional fluctuations that occur in some modulated structures. Thus, we believe that electron microscopy in its various modes will provide great insight into these interesting aspects of mineral structures.

The information available commonly contains uncertainties and is usually insufficient to specify completely the details of modulated structures. For systems that are well ordered over large volumes, X-ray diffraction is the method of choice. However, for many systems, especially ones where structural

variations are highly localized and not perfectly periodic, electron optical methods are desirable. For some systems they provide the only feasible approach (*e.g.*, Sharma and Khilborg, 1981; Veblen and Buseck, 1979a), and the refinement and quantifying of these methods appears to be the best way to further our knowledge for many important systems.

The terminology that is summarized in Table 1 and that we have used here for modulated and intergrowth structures is certainly subject to further refinements. However, it appears to be preferable to the more general usage of Cowley *et al.* (1979), in which the term "modulated structures" was used to include all long-period ordered structures and even some structures having only short-range order.

There remains an uncertain area of terminology concerning the distinction between commensurately modulated structures and superstructures. It is, perhaps, sufficient to suggest that a commensurately modulated structure is one that, for different values of temperature, composition, or other parameters, could easily be incommensurate. This can be envisaged for either the long-wavelength, atom-displacement modulations, or for those cases where the modulation periodicity is given statistically as the average spacing of a structural discontinuity or the average periodicity of a compositional variation. However, complications can arise because both nominally commensurate superstructures and modulated structures can be imperfectly ordered. The presence of faults in a superstructure can result in the apparent displacement of diffraction spots from their regular reciprocal lattice positions, suggesting an incommensurate structure. The spots resulting from a long-range periodicity may be blurred or streaked. In such cases there is no substitute for the direct imaging methods of electron microscopy for sorting out the confusion.

Acknowledgments

References

Bando, Y. and Iijima, S. (1980) An incommensurate superstructure of hexagonal tungsten bronze. In G. W. Bailey, Ed., 38th Annual Proceedings Electron Microscopy Society of America, p. 166–167, San Francisco, California.

Bursill, L. A. and Grzinic, G. (1980) Incommensurate superlattice ordering in the hollandites $Ba_xTi_{8-x}Mg_xO_{16}$ and $Ba_x Ti_{8-2x}Ga_{2x}O_{16}$. Acta Crystallographica, B36, 2902–2913.

Buseck, P. R. and Veblen, D. R. (1981) Defects in minerals as observed with high-resolution transmission electron microscopy. Bulletin de la Société Francaise de Minéralogie et de Cristallographie, 104, 249–260.

Cowley, J. M. (1979) Retrospective introduction: What are modulated structures? In J. M. Cowley et al., Eds., Modulated Structures—1979, p. 3–9, American Institute of Physics, New York.

Cowley, J. M. (1981a) Coherent convergent-beam electron microdiffraction. Kristallografiya, 26, 965–973.

Cowley, J. M. (1981b) Coherent interference effects in STEM and CBED. Ultramicroscopy, 7, 19–26.

Cowley, J. M., Cohen, J. B., Salamon, M. B., and Wuensch, B. J. (1979) Modulated Structures—1979. American Institute of Physics, New York.

Cowley, J. M. and Fields, P. M. (1979) Dynamical theory for electron scattering from crystal defects and disorder. Acta Crystallographica, A 35, 28–37.

Dollase, W. A. (1967) The crystal structure at 220°C of orthorhombic high tridymite from the Steinbach meteorite. Acta Crystallographica, 23, 617–623.

Eggleton, R. A. and Buseck, P. R. (1980) The orthoclase-microcline inversion: A high-resolution transmission electron microscope study and strain analysis. Contributions to Mineralogy and Petrology, 74, 123–133.

Goldsmith, J. R. and Laves, F. (1954) Potassium feldspars structurally intermediate between microcline and sanidine. Geochimica et Cosmochimica Acta, 6, 100–118.

Goodman, P. and Lehmpfuhl, G. (1968) Observation of the breakdown of Friedel's Law in electron diffraction and symmetry determination from zero-layer interactions. Acta Crystallographica, A24, 339–347.

Grey, I. E. and Bursill, L. A. (1978) High-temperature intergrowth structures in the Fe_2O_3–TiO_2 system–metal atom ordering in the intergrowth boundaries. Acta Crystallographica, B34, 2412–2424.

Gunderson, S. H. and Wenk, H. R. (1981) Heterogeneous microstructures in oolitic carbonates. American Mineralogist, 66, 789–800.

Horst, W., Tagai, T., Korekawa, M. and Jagodzinski, H. (1981) Modulated structure of a plagioclase An_{52}: Theory and structure determination. Zeitschrift für Kristallographie, 157, 233–250.

Hutchison, J. L., Anstis, G. R., Humphreys, C. J. and Ourmazd, A. (1982) Atomic images of silicon and related materials; fact or artefact? In M. G. Goringe, Ed., Electron Microscopy and Analysis (1981), p. 357–360. The Institute of Physics, Bristol and London.

Hyde, B. G. (1976) Rutile: Planar defects and derived structures. In H.-R. Wenk, Ed., Electron Microscopy in Mineralogy, p. 310–318. Springer Verlag, Berlin.

Hyde, B. G. (1979) Some modulation operations and derived structures. In J. M. Cowley et al., Eds., Modulated Structures—1979, p. 87–98. American Institute of Physics, New York.

Iijima, S. (1975) High-resolution electron microscopy of crystallographic shear structures in tungsten oxides. Journal of Solid

State Chemistry, 14, 52–65.

Kihlborg, L., Sundberg, M. and Hussain, A. (1980) Defects in intergrowth tungsten bronzes formed by vapour transport or subjected to partial oxidation. Chemica Scripta, 15, 182–186.

Koto, K. and Morimoto, N. (1975) Superstructure investigation of bornite, Cu_5FeS_4, by the modified partial Patterson function. Acta Crystallographica, B31, 2268–2273.

Kunze, G. (1956) Die gewellte Struktur des Antigorits, I. Zeitschrift für Kristallographie, 108, 82–107.

Liliental, Z., Carpenter, R. W. and Pollack, S. (1981) CBED identification of type 3C pyrrhotite in coal liquefaction product. In G. W. Bailey, Ed., 39th Annual Proceedings Electron Microscopy Society of America, p. 360–361, Atlanta, Georgia.

McConnell, J. D. C. (1971) Electron optical study of phase transformations. Mineralogical Magazine, 38, 1–120.

Magnéli, A. (1953) Studies on the hexagonal tungsten bronzes of potassium, rubidium and cesium. Acta Chemica Scandinavica, 7, 315–324.

Makovicky, E. and Hyde, B. G. (1979) On modulated, noncommensurate layer structures (nomenclature and classification). In J. M. Cowley et al., Eds., Modulated Structures—1979, p. 99–101. The American Institute of Physics, New York.

Mihama, K. (1971) Growth and structure of AuCu-II particles. Journal of the Physical Society of Japan, 31, 1677.

Miúra, Y. (1979) Modulated microstructure of plagioclase feldspars from Hida, Hidaka and Abukuma metamorphic rocks of Japan. In J. M. Cowley et al., Eds., Modulated Structures—1979, p. 314–316. The American Institute of Physics, New York.

Morimoto, N. (1964) Structures of two polymorphic forms of Cu_5FeS_4. Acta Crystallographica, 17, 351–360.

Morimoto, N. (1978) Incommensurate superstructures in tranformation of minerals. Recent Progress of Natural Sciences in Japan, 3, 183–206.

Morimoto, N. (1979) The modulated structures of feldspars. In J. M. Cowley et al., Eds., Modulated Structures—1979, p. 299–310. The American Institute of Physics, New York.

Morimoto, N. and Kullerud, G. (1966) Polymorphism on the Cu_5FeS_4–Cu_9S_5 join. Zeitschrift für Kristallographie, 123, 235–254.

Nakazawa, H., Morimoto, N. and Watanabe, E. (1976) Direct observation of iron vacancies in polytypes of pyrrhotite. In H.-R. Wenk et al., Eds., Electron Microscopy in Mineralogy, p. 304–309. Springer-Verlag, Berlin.

Nukui, A., Yamamoto, A. and Nakazawa, H. (1979) Nonintegral phase in tridymite. In J. M. Cowley et al., Eds., Modulated Structures—1979, p. 327–329. The American Institute of Physics, New York.

Pierce, L. (1979) High Resolution Electron Microscopy of Sulfides. Ph.D. Dissertation, Arizona State University, Arizona.

Pierce, L. and Buseck, P. R. (1974) Electron imaging of pyrrhotite superstructures. Science, 186, 1209–1212.

Pierce, L. and Buseck, P. R. (1976) A comparison of bright field and dark field imaging of pyrrhotite structures. In H.-R. Wenk et al., Eds., Electron Microscopy in Mineralogy, p. 137–141. Springer-Verlag, Berlin.

Pierce, L. and Buseck, P. R. (1978) Superstructuring in the bornite–digenite series: A high-resolution electron microscopy study. American Mineralogist, 63, 1–16.

Post, J. E., Von Dreele, R. B. and Buseck, P. R. (1982)

Symmetry and cation displacements in hollandites: Structure refinements of hollandite, cryptomelane and priderite. Acta Crystallographica, B38, 1056–1065.

Putnis, A. and Grace, J. (1976) The transformation behaviour of bornite. Contributions to Mineralogy and Petrology, 55, 311–315.

Reeder, R. J. (1981) Electron optical investigation of sedimentary dolomites. Contributions to Mineralogy and Petrology, 76, 148–157.

Reeder, R. J. and Nakajima, Y. (1982) The nature of ordering defects in dolomite. Physics and Chemistry of Minerals, 8, 29–35.

Reeder, R. J. and Wenk, H. R. (1979) Microstructures in low temperature dolomites. Geophysical Research Letters, 6, 77–80.

Sharma, R. and Kihlborg, L. (1981) Structures and defects of new intergrowth tungsten bronze analogues revealed by high resolution electron microscopy. Material Research Bulletin, 16, 377–380.

Shindo, D. (1982) High resolution images of ordered alloys by high voltage electron microscopy. Acta Crystallographica, A38, 310–317.

Smith, J. V. (1974) Feldspar Minerals. Vol. 1. Crystal Structure and Physical Properties. Springer-Verlag, Berlin, Chap. 5.

Spinnler, G. E., Veblen, D. R. and Buseck, P. R. (1982) Complexities in antigorite modulations (abst.). Geological Society of America Abstracts with Programs, 14, 623.

Steeds, J. W. (1979) Convergent beam electron diffraction. In J. J. Hren et al., Eds., Introduction to Analytical Electron Microscopy, p. 387–422. Plenum Press, New York.

Taftø, J. (1979) Channelling effects in electron induced X-ray emission from diatomic crystals. Zeitschrift für Naturforschung, 34a, 452–458.

Tomeoka, K., Buseck, P. R., and Ohmasa, M. (1981) Electron microscopy of the modulated structure of $Cu_3Bi_5S_9$ (abstr.) Geological Society of American Abstracts with Programs, 13, 568.

Tomeoka, K., and Ohmasa, M. (1982) The modulated structure of cubic Cu_9BiS_6. American Mineralogist, 67, 360–372.

Tu, K. N. and Howie, A. (1978) Forbidden 200 diffraction spots in silicon. Philosophical Magazine, B 37, Vol. 1, 73–81.

Veblen, D. R. and Buseck, P. R. (1979a) Chain-width order and disorder in biopyriboles. American Mineralogist, 64, 687–700.

Veblen, D. R. and Buseck, P. R. (1979b) New ordering schemes in mixed-chain silicates. In J. M. Cowley et al., Eds., Modulated Structures—1979, p. 321–323. American Institute of Physics, New York.

Veblen, D. R. and Buseck, P. R. (1979c) Serpentine minerals: Intergrowths and new combination structures. Science, 206, 1398–1400.

Veblen, D. R. and Buseck, P. R. (1981) Hydrous pyriboles and sheet silicates in pyroxenes and uralites: Intergrowth microstructures and reaction mechanisms. American Mineralogist, 66, 1107–1134.

Watanabe, D. (1979) Long period antiphase structures in ordered alloys. In J. M. Cowley et al., Eds., Modulated Structures—1979, p. 229–239. The American Institute of Physics, New York.

Wenk, H.-R. and Nakajima, Y. (1979) Periodic superstructures in calcic plagioclase. In J. M. Cowley et al., Eds., Modulated Structures—1979, p. 317–320. The American Institute of Phys-

ics, New York.

Wuensch, B. J. (1979) Superstructures in sulfide minerals. In
J. M. Cowley *et al.*, Eds., Modulated Structures—1979. p.
337–354. The American Institute of Physics, New York.

Yada, K. (1979) Microstructures of chrysotile and antigorite by
high-resolution electron microscopy. Canadian Mineralogist,
17, 679–691.